

Numerical simulations of gravitational collapse in Einstein-aether theory

David Garfinkle*

Department of Physics, Oakland University, Rochester, MI 48309

Christopher Eling[†] and Ted Jacobson[‡]

Department of Physics, University of Maryland, College Park, MD 20742

We study gravitational collapse of a spherically symmetric scalar field in Einstein-aether theory (general relativity coupled to a dynamical unit timelike vector field). The initial value formulation is developed, and numerical simulations are performed. The collapse produces regular, stationary black holes, as long as the aether coupling constants are not too large. For larger couplings a finite area singularity occurs. These results are shown to be consistent with the stationary solutions found previously.

PACS numbers: 04.50.+h,04.70.Bw,04.25.Dm

I. INTRODUCTION

Over the past several years there has been a renewal of interest in the physics of Lorentz symmetry violation. These investigations are largely motivated by the enduring problem of quantum gravity and also cosmological mysteries such as the dark matter and dark energy problems. Lorentz violation (LV) effects in Standard Model extensions and modified particle dispersion relations are currently tightly constrained by high precision tests [1], however constraints on gravitational LV effects are not as severe. Various approaches to incorporating LV into gravity have been investigated, see for example Refs. [2, 3, 4, 5, 6, 7, 8, 9, 10, 11, 12, 13, 14].

In this paper we will consider “Einstein-aether” theory (or ae-theory, for short) [6, 15], which consists of a dynamical unit timelike vector field u^a coupled to Einstein gravity. The u^a “aether” field can be thought of as the 4-velocity of a preferred frame. The LV here is a form of spontaneous symmetry breaking, since the unit timelike constraint requires the vector field to have a non-zero value everywhere in any solution, even flat spacetime.

The Lagrangian of ae-theory depends on four dimensionless coupling constants $c_{1,2,3,4}$. By studying the phenomenology of ae-theory it can be compared with observations in order to constrain the c_i values and possibly rule the theory out entirely as a description of nature. Observational constraints on ae-theory have been determined from parameterized post-Newtonian analysis [16, 17, 18], stability and energy positivity [19, 20, 21, 22], primordial nucleosynthesis [23], and vacuum Cerenkov radiation [21]. The combined constraints from all of these are reviewed in Ref. [18]. They are all consistent with a large (order unity) 2d region in the 4d parameter space. Agreement with weak field radiation damping (such as in binary pulsar systems) [24, 25] is expected to restrict the

parameters to a narrow band of width $\sim 10^{-3}$ in that 2d region, and combined constraints from many such systems may further narrow the allowed region to a small neighborhood of the origin, with size of order 10^{-1} - 10^{-2} .

It is likely that theories with LV can generally be more tightly constrained by examining strong field solutions. In addition, the properties of such solutions may also be of interest from a purely mathematical physics perspective since the additional fields that couple to GR can produce interesting new sorts of solutions and phenomena. Black hole solutions have been considered in the ghost condensate theory [26], and spherically symmetric solutions in the relativistic MOND theory were studied in [27]. Work on this subject in ae-theory was begun long ago in special cases [3, 4, 6], and a study of the solutions for general values of the coupling parameters was completed recently in [28] and [29].

In these papers the time independent spherically symmetric solutions in ae-theory were characterized by examining the field equations as a set of coupled ordinary differential equations. It was demonstrated that there is generically a three parameter family of solutions to these equations. Imposing the boundary condition of asymptotic flatness at spatial infinity reduces the solution space to a two parameter family. This differs from GR, in which there is a unique spherically symmetric solution, the Schwarzschild metric, which is automatically asymptotically flat. The one parameter subset of solutions where u^a is aligned with the timelike Killing vector was found analytically and discussed in detail in [28]. It was also shown that this solution describes the exterior of a static fluid star.

Regular black holes in ae-theory must be described by a different solution, since the aether is a timelike vector so it cannot coincide with the Killing vector which is null on the horizon and spacelike inside. That is, the aether must be flowing into the black hole. Moreover, the theory possesses spin-2, spin-1, and spin-0 “massless” wave modes that travel at speeds that differ from one another and from the metric speed of light [19]. To qualify as a black hole, a solution must therefore contain a re-

*Electronic address: garfinkl@oakland.edu

[†]Electronic address: cting@physics.umd.edu

[‡]Electronic address: jacobson@umd.edu

gion where all of these wave modes are trapped. It was found in [29] that in spherical symmetry, regularity at the metric, spin-2, and spin-1 horizons is automatic, but regularity at the spin-0 horizon is a supplementary condition. This condition reduces the two-parameter family of asymptotically flat solutions to a one-parameter family characterized by the total mass or horizon area. Particular black hole solutions with regular spin-0 horizons were found by numerical integration for special cases of the coupling parameters. Like the Schwarzschild solution, these solutions have spacelike singularities at the origin, and in the exterior the metric functions are very close to the familiar Schwarzschild solution, even for fairly large coupling constants c_i . (The differences become more pronounced in the black hole interior.) For certain large values of the coupling constants no black hole solution with a regular spin-0 horizon was found.

From an astrophysical point of view, an important question is which solutions describe the final state of a gravitational collapse of matter fields. In [29] it was conjectured that the solutions with regular spin-0 horizons—when they exist—are the ones that arise from collapse of initially nonsingular data. The main objective of this paper is to test that conjecture by numerical evolution of the time dependent spherically symmetric field equations given appropriate collapsing initial data. A massless scalar field coupled only to the metric will serve as the matter field.

In Section II we review the nature and status of Einstein-aether theory, and discuss the nature of black holes in this theory. Section III together with the Appendix develops the initial value formulation under the assumption that the aether vector is hypersurface orthogonal, as is always the case in spherical symmetry. The results of numerical collapse simulations are presented in Section IV. We find that the collapsing scalar field does indeed reach a final stationary black hole state with a regular spin-0 horizon, for the range of coupling constants found in [29] to allow such states. Outside this range of c_i we find solutions that develop a finite area singularity at the would-be spin-0 horizon. The numerical evolution procedure also allows for wider explorations of space of c_i than was done in [29]. The results appear to support the conjecture that formation of black holes with regular spin-0 horizons is generic in ae-theory for coupling parameters that are not too large.

II. EINSTEIN-AETHER THEORY

The action for Einstein-aether theory is the most general generally covariant functional of the spacetime metric g_{ab} and aether field u^a involving no more than two derivatives (not including total derivatives),

$$S = \int \sqrt{-g} (L_{\text{ae}} + L_{\text{matter}}) d^4x \quad (1)$$

where

$$L_{\text{ae}} = \frac{1}{16\pi G} [R - K^{ab}{}_{mn} \nabla_a u^m \nabla_b u^n + \lambda (g_{ab} u^a u^b + 1)] \quad (2)$$

and L_{matter} denotes the matter lagrangian. Here R is the Ricci scalar, $K^{ab}{}_{mn}$ is defined as

$$K^{ab}{}_{mn} = c_1 g^{ab} g_{mn} + c_2 \delta_m^a \delta_n^b + c_3 \delta_n^a \delta_m^b - c_4 u^a u^b g_{mn} \quad (3)$$

where the c_i are dimensionless coupling constants, and λ is a Lagrange multiplier enforcing the unit timelike constraint on the aether. The convention used in this paper for metric signature is $(-+++)$ and the units are chosen so that the speed of light defined by the metric g_{ab} is unity. In the weak-field, slow-motion limit ae-theory reduces to Newtonian gravity [23], with a value of Newton's constant G_N related to the parameter G in the action (1) by $G_N = G(1 - (c_1 + c_4)/2)^{-1}$.

In this paper we take the matter field to be a minimally coupled massless scalar field χ , with Lagrangian $-\nabla_a \chi \nabla^a \chi$. However, to simplify the form of the equations of motion, we introduce the quantity $\psi = \chi \sqrt{16\pi G}$ so that the matter Lagrangian takes the form

$$L_{\text{matter}} = \frac{-1}{16\pi G} \nabla_a \psi \nabla^a \psi. \quad (4)$$

The field equations from varying (1) with respect to g^{ab} , u^a , ψ , and λ are given respectively by

$$G_{ab} = T_{ab} \quad (5)$$

$$\nabla_a J^a{}_b + \lambda u_b + c_4 a_a \nabla_b u^a = 0 \quad (6)$$

$$\nabla^a \nabla_a \psi = 0 \quad (7)$$

$$u^a u_a = -1. \quad (8)$$

Here G_{ab} is the Einstein tensor of the metric g_{ab} ; and the quantities $J^a{}_b$, a_a and the stress-energy T_{ab} are given by

$$J^a{}_m = K^{ab}{}_{mn} \nabla_b u^n \quad (9)$$

$$a_a = u^b \nabla_b u_a \quad (10)$$

$$\begin{aligned} T_{ab} = & -\frac{1}{2} g_{ab} (J^c{}_d \nabla^d u^c + \nabla_c \psi \nabla^c \psi) \\ & + \nabla_a \psi \nabla_b \psi + c_4 a_a a_b + \lambda u_a u_b \\ & + c_1 (\nabla_a u_c \nabla_b u^c - \nabla^c u_a \nabla_c u_b) \\ & + \nabla_c [J^c{}_{(a} u_{b)} + u^c J_{(ab)} - J_{(a}{}^c u_{b)}]. \end{aligned} \quad (11)$$

In this paper we will perform numerical simulations of this system in spherical symmetry. The condition of spherical symmetry implies that the twist $\omega_a = \epsilon_{abcd} u^b \nabla^c u^d$ of the vector field u^a vanishes. This makes the four parameters of the Lagrangian redundant: the action depends only on c_2 , c_{13} and c_{14} where we use the abbreviation c_{13} to stand for $c_1 + c_3$ (and correspondingly for c_{14}). (In Ref. [29] it is shown that when the twist vanishes the c_4 term can be absorbed by the shifts $c_1 \rightarrow c_1 + c_4$ and $c_3 \rightarrow c_3 - c_4$. Thus the action depends only on c_2 , c_{14} and $c_3 - c_4$. But since the latter is equal to $c_{13} - c_{14}$, the action is also determined by c_2 , c_{13} , and

c_{14} .) Because the twist vanishes, it follows that u^a is hypersurface orthogonal.

For our study of scalar field collapse we considered a case where the parameters c_i satisfy the requirements that (i) the Einstein-aether theory has precisely the same post-Newtonian parameters as general relativity, so it agrees in the post-Newtonian approximation with all experimental tests of general relativity, (ii) the theory is linearly stable, (iii) the wave modes all carry positive energy, and (iv) the wave modes travel at greater than or equal to the matter speed of light, so there is no vacuum Čerenkov radiation. Together these impose the conditions [18]

$$c_2 = \frac{c_3^2}{3c_1} - \frac{2c_1 + c_3}{3} \quad (12)$$

$$c_4 = \frac{-c_3^2}{c_1} \quad (13)$$

$$0 < c_{13} < 1 \quad (14)$$

$$0 < (c_1 - c_3) < \frac{c_{13}}{3(1 - c_{13})}. \quad (15)$$

We chose $c_1 = 1/3$ and $c_3 = 1/6$ (essentially in the midrange of the inequalities given above) and then determined c_2 and c_4 by the above equalities. This yields the parameter set

$$c_1 = \frac{1}{3}, \quad c_2 = -\frac{1}{4}, \quad c_3 = \frac{1}{6}, \quad c_4 = -\frac{1}{12}. \quad (16)$$

This choice of the constants c_i is different from those used in the studies of static black holes in [29]. However, for the Einstein-aether theory without matter, the transformation $u_a \rightarrow \sqrt{\sigma}u_a$ (with σ a constant and with h_{ab} remaining unchanged) takes Einstein-aether theory into itself but with changes in the parameters c_i [30]. This transformation and the restriction to spherical symmetry allows one to transform the results with our parameter choice (16) to one with c_{13} and c_4 vanishing and with $c_1 = 1/4$ and $c_2 = 1/2$. This new set of parameters falls in the class that lends itself to a numerical integration of the static, spherically symmetric Einstein-aether equations using the methods of [29], and thus allows a direct comparison of a static solution with the end state of our numerical simulations of gravitational collapse.

In this paper we examine the collapse process to determine the nature of the black hole that is formed. This issue is somewhat more subtle in Einstein-aether theory than in general relativity. Usually in a gravitational collapse simulation one looks for apparent horizons: marginally outer trapped surfaces of the metric g_{ab} . Typically the spacetime outside the apparent horizon settles down to a stationary (static in the spherically symmetric case) black hole. However, Einstein-aether theory contains a spin-0 mode that travels at the speed v_0 where [19]

$$v_0^2 = \frac{c_{123}(2 - c_{14})}{c_{14}(1 - c_{13})(2 + c_{13} + 3c_2)}. \quad (17)$$

For the equalities that we have imposed on the c_i this expression reduces to

$$v_0^2 = \frac{c_{13}}{3(c_1 - c_3)(1 - c_{13})}. \quad (18)$$

Thus, the boundary of the black hole should be a horizon that just barely traps the spin-0 mode. This turns out to be equivalent to a marginally outer trapped surface of the metric $\tilde{g}_{ab} = g_{ab} + (1 - v_0^2)u_a u_b$. Thus in searching for black holes we look for marginally outer trapped surfaces of the metric \tilde{g}_{ab} , which for brevity we will call spin-0 horizons. For the parameter choice (16), the spin-0 speed from (18) is $\sqrt{2}$, so the spin-0 horizon lies inside the metric horizon.

III. INITIAL VALUE FORMULATION

Numerical evolution requires a choice of the surfaces of constant time, and we will choose those surfaces orthogonal to u^a . This choice is always possible in spherical symmetry since u^a is necessarily hypersurface orthogonal. The spatial metric h_{ab} and extrinsic curvature K_{ab} of these hypersurfaces are then given by

$$h_{ab} = g_{ab} + u_a u_b \quad (19)$$

$$K_{ab} = -\frac{1}{2}\mathcal{L}_u h_{ab} \quad (20)$$

where \mathcal{L} denotes Lie derivative. Notice that the constraint (8) that u^a be a unit vector is built into our initial value formulation by its identification with the unit normal.

The use of K_{ab} as a variable allows us to write Einstein's equation in a form that is first order in time. Similarly we introduce the quantity $P = \mathcal{L}_u \psi$ which allows us to do the same for the wave equation.

The time evolution vector field takes the form $t^a = \alpha u^a + \beta^a$. We use as a radial coordinate r the length in the radial direction (rather than an area coordinate). This makes the spatial metric

$$h_{ab} = \partial_a r \partial_b r + \Phi^2 \Sigma_{ab} \quad (21)$$

where Σ_{ab} is the unit two-sphere metric.

The quantities that are evolved are (ψ, P, K, a_r, Φ) . All other quantities are found from these. In the appendix, equations of motion for these quantities are derived from the Euler-Lagrange equations (5-8). These equations are

$$\partial_t \psi = \alpha P + \beta^r \partial_r \psi \quad (22)$$

$$\begin{aligned} \partial_t P &= \beta^r \partial_r P \\ &+ \alpha \left[PK + a^r \partial_r \psi + \partial_r \partial_r \psi + \frac{2\partial_r \Phi}{\Phi} \partial_r \psi \right] \end{aligned} \quad (23)$$

$$\begin{aligned} \partial_t K &= \beta^r \partial_r K + \frac{\alpha}{3} K^2 \\ &+ \frac{\alpha}{2 + c_{13} + 3c_2} \left[(c_{14} - 2)(\partial_r a_r + 2a_r \partial_r \Phi / \Phi + a_r a_r) \right] \end{aligned}$$

$$+ 2P^2 + 3(1 - c_{13})Q^2 \Big] \quad (24)$$

$$\begin{aligned} \partial_t a_r &= \beta^r \partial_r a_r + \alpha \left[\left(\frac{2K}{3} - Q \right) a_r \right. \\ &\quad \left. + \frac{c_{13}}{c_{14}(1 - c_{13})} P \partial_r \psi - \frac{c_{123}}{c_{14}(1 - c_{13})} \partial_r K \right] \end{aligned} \quad (25)$$

$$\partial_t \Phi = \beta^r \partial_r \Phi + \alpha \Phi (Q/2 - K/3). \quad (26)$$

Here $Q = K^r_r - (K/3)$ is the trace-free part of the extrinsic curvature. As shown in the appendix, the quantities Q , α and β are determined by

$$\begin{aligned} \partial_r Q &= -\frac{3Q}{\Phi} \partial_r \Phi + (1 - c_{13})^{-1} \left[\frac{1}{3}(2 + c_{13} + 3c_2) \partial_r K \right. \\ &\quad \left. - P \partial_r \psi \right] \end{aligned} \quad (27)$$

$$\partial_r \ln \alpha = a_r \quad (28)$$

$$\partial_r \beta^r = \alpha(Q + K/3). \quad (29)$$

The Hamiltonian initial value constraint is

$$\begin{aligned} \mathcal{C} &= \partial_r \partial_r \Phi + \frac{(\partial_r \Phi)^2 - 1}{2\Phi} + c_{14} a_r \partial_r \Phi \\ &\quad + \frac{\Phi}{4} \left[c_{14} (2\partial_r a_r + a_r a_r) + P^2 + (\partial_r \psi)^2 \right. \\ &\quad \left. + \frac{3}{2}(1 - c_{13})Q^2 - \frac{1}{3}(2 + c_{13} + 3c_2)K^2 \right] \\ &= 0. \end{aligned} \quad (30)$$

For initial data, we choose a moment of time symmetry, so that P, Q and K are zero. Both a_r and ψ can be freely specified. We choose a_r to vanish and ψ to be

$$\psi = a_0 \exp[-(r^2 - r_0^2)^2 / s^4] \quad (31)$$

where a_0, r_0 and s are constants. Thus the scalar field is initially at rest and is essentially a spherical shell of radius r_0 , thickness s and amplitude a_0 . Then equation (30) is integrated outwards to find Φ , subject to the boundary conditions $\Phi = 0$ and $\partial_r \Phi = 1$ at $r = 0$. The other boundary conditions that need to be imposed are $\beta^r = 0$ and $Q = 0$ for smoothness at $r = 0$, and $\alpha \rightarrow 1$ for a gauge fixing as $r \rightarrow \infty$.

The evolution proceeds as follows: given (ψ, P, K, a_r, Φ) at one time step, equations (28) and (27) are integrated to find α and Q . Then equation (29) is integrated to find β^r . Then equations (22), (23), (24), (25) and (26) are used to find respectively (ψ, P, K, a_r, Φ) at the next time step. Since Φ is evolved using equation (26) but must also satisfy equation (30) this means that equation (30) can be used as a code check in a convergence test.

IV. NUMERICAL RESULTS

The specific parameters we used for the initial scalar field are $a_0 = 0.15$, $r_0 = 10$ and $s = 4$. Initial data with

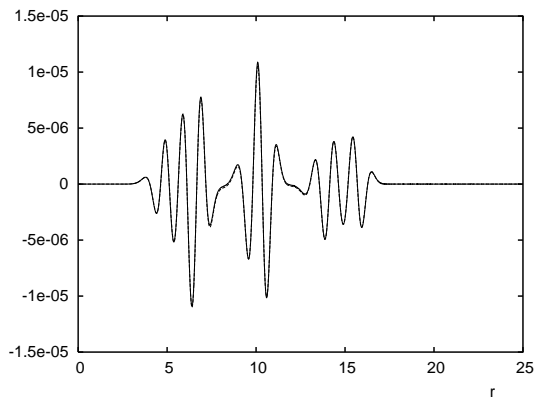


FIG. 1: Plot of \mathcal{C} vs r for a simulation with 12800 points (solid line) and $\mathcal{C}/4$ for a simulation with 6400 points (dashed line). The agreement of the two curves demonstrates second order convergence of the code. The curves are for a time when the scalar field is in the process of collapsing.

these parameters leads to gravitational collapse and the formation of a black hole.

In the numerical simulations spatial derivatives were implemented with standard centered finite differences. The time evolution was done with the Iterated Crank-Nicholson (ICN) method. Kreiss-Oliger type dissipation was used for stability. The first grid point was at $r = 0$. Of the quantities that are evolved by the code, smoothness requires that a_r and Φ are odd functions of r and that the other quantities are even. The code evolves the quantities on all grid points except the first and last. The odd quantities are set to zero on the first grid point, while the even quantities are set as follows:

$$f_1 = (4f_2 - f_3)/3 \quad (32)$$

which implements the condition that the derivative of f vanish at the origin. Here f denotes any even quantity, and the subscript denotes the corresponding gridpoint. At the last gridpoint, N , all the evolved quantities are set to zero with the exception of Φ which is set by

$$\Phi_N = 2\Phi_{N-1} - \Phi_{N-2} \quad (33)$$

which is the appropriate boundary condition for a quantity that asymptotically satisfies $\partial\Phi/\partial r = 1$.

The simulations were run on a SunBlade 2000 in double precision. The number N of gridpoints used was 12800 and the initial value of r at the outermost gridpoint was 80. Figure (1) shows the result of a convergence test of the code. It is a plot of the constraint quantity \mathcal{C} of equation (30) done at a time when the scalar field is in the process of collapsing. The solid curve represents \mathcal{C} for a simulation with 12800 points, while the dashed curve represents $\mathcal{C}/4$ for a simulation with 6400 points. The fact that the two curves agree demonstrates that the code is second order convergent.

The simulations show that for the initial data used the collapse does form a spin-0 horizon (which is contained

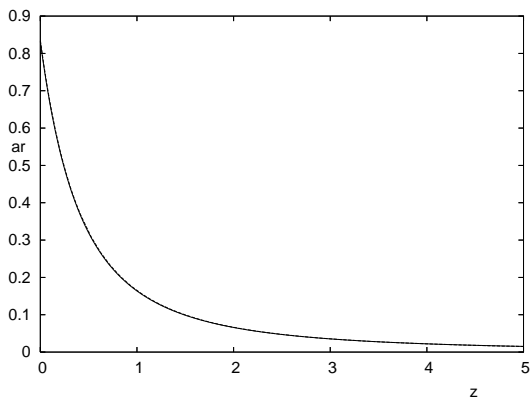


FIG. 2: Plot of a_r vs z for the end state of the collapse simulation (solid line) and the static solution found using the method of [29] (dashed line)

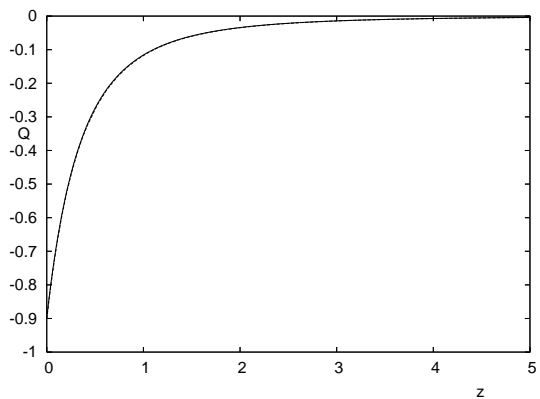


FIG. 4: Plot of Q vs z for the end state of the collapse simulation (solid line) and the static solution found using the method of [29] (dashed line)

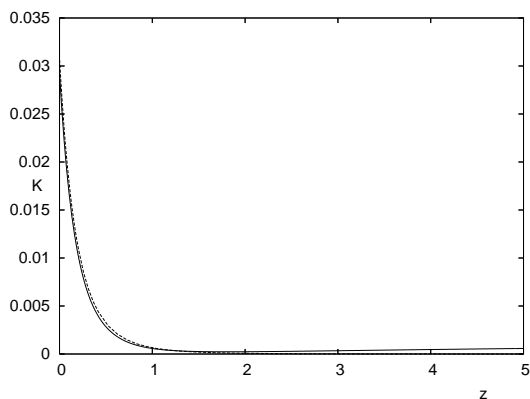


FIG. 3: Plot of K vs z for the end state of the collapse simulation (solid line) and the static solution found using the method of [29] (dashed line)

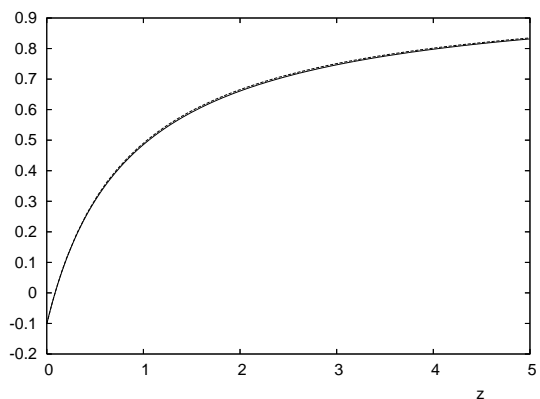


FIG. 5: Plot of $\nabla^a \Phi \nabla_a \Phi$ vs z for the end state of the collapse simulation (solid line) and the static solution found using the method of [29] (dashed line)

within an ordinary horizon, that is a marginally outer trapped surface of the metric g_{ab}). Furthermore, outside of the spin-0 horizon the metric and aether field do settle down into a time independent state. In addition, all the scalar field either falls into the black hole or escapes, so that near the horizon the time independent state is that of a pure Einstein-aether black hole with no matter other than the aether field u^a . We are able to follow the time evolution to late times with our horizon crossing time slices, orthogonal to the timelike aether field u^a , because the lapse α is driven to zero as the singularity is approached. The reason for this can be traced to Eqn. (28). Evidently at the singularity the aether acceleration component a_r goes to positive infinity.

In reference [29] the static black holes of Einstein-aether theory with a regular spin-0 horizon were found numerically, and it was conjectured that these would be the endstates of gravitational collapse. Our simulations verify that this is indeed what happens. In figures (2), (3) and (4) are plotted respectively the quantities a_r , K and Q for this simulation (solid line) and for the static so-

lution found using the method of [29] (dashed line). Here the static solution is found using the transformed choice of the parameters c_i , and its metric and aether variables are then transformed back as explained in Section II to make the comparison with the result of the collapse simulation. In all cases the quantities are plotted as functions of $z = \Phi - \Phi_0$ where Φ_0 is the value of Φ at the spin-0 horizon. Note that the agreement is extremely good, so the end result of collapse is indeed the static black hole solution found using the method of [29].

The quantities a_r , K and Q completely determine the aether field, and since we are treating spherically symmetric spacetimes where there are no separate gravitational degrees of freedom, these quantities also completely determine the metric. Nonetheless, it is helpful to do a direct comparison of the metric of the endstate of the collapse simulation and the static metric found using the method of [29]. For a static, spherically symmetric metric with area radius Φ , the metric is determined by the quantities $\nabla_a \Phi \nabla^a \Phi$ and $\nabla_a \nabla^a \Phi$. In figures (5) and (6) these quantities are respectively plotted. As with

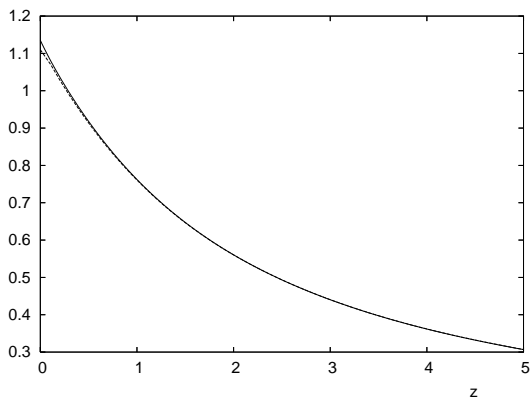


FIG. 6: Plot of $\nabla^a \nabla_a \Phi$ vs z for the end state of the collapse simulation (solid line) and the static solution found using the method of [29] (dashed line)

figures (2-4) the quantities are plotted as functions of z with the endstate of the collapse simulation as a solid line and the static metric found using the method of reference [29] as a dashed line. The agreement between the curves shows that the metric in the final state of the collapse simulation agrees with the static metric.

We now present the results of a slightly different simulation that uses directly a different parameter choice of [29], namely $c_3 = c_4 = 0$, and c_2 chosen so that the spin-0 horizon coincides with the usual metric horizon. That is, the speed v_0 in (17) is set equal to one, which requires

$$c_2 = \frac{-c_1^3}{2 - 4c_1 + 3c_1^2}. \quad (34)$$

If $0 < c_1 < 1$ such theories meet all the linear stability conditions (stable modes, positive energy, and no vacuum Čerenkov radiation). In this class the post-Newtonian preferred frame parameter α_1 vanishes identically, but α_2 does not vanish unless $c_1 = 2/3$ (see [17, 18] for $\alpha_{1,2}$). Nevertheless, since the stability conditions are met, it seems likely that the behavior of collapse in the theory is qualitatively similar to the previous case where also α_2 vanishes. In [29], static, asymptotically flat black hole solutions were found in the range $c_1 \leq 0.7$, by integrating from a regular horizon to spatial infinity using a shooting method. The asymptotically flat boundary condition could not be met for $c_1 \geq 0.8$.

We performed collapse simulations for the case $c_1 = 0.7$ and the case $c_1 = 0.8$. In the $c_1 = 0.7$ case a regular horizon forms. However, in the $c_1 = 0.8$ case, no horizon forms and the evolution seems to become singular, thus indicating the formation of a naked singularity. Figure (7) Shows the value of K (dashed line) for the $c_1 = 0.8$ simulation at a time shortly before the singularity forms. For comparison, the same figure shows (solid line) the value of K at the same time for the $c_1 = 0.7$ simulation. Since the collapse solutions are by construction asymptotically flat, this is consistent with what was found for static solutions in [29].

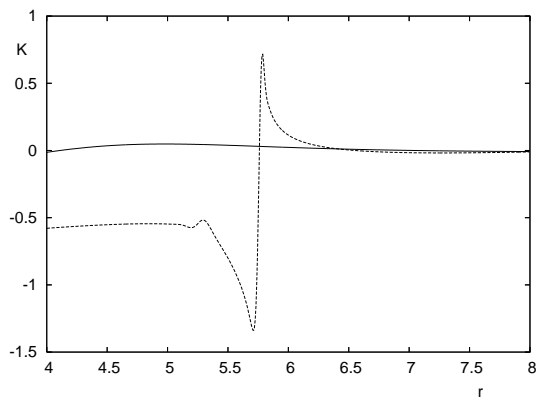


FIG. 7: Plot of K vs r for simulations with $c_1 = 0.7$ (solid line) and $c_1 = 0.8$ (dashed line).

V. CONCLUDING REMARKS

We have examined the process of dynamical collapse of a spherically symmetric, self-gravitating scalar field pulse in Einstein-aether theory. In pure Einstein gravity it is well known that for appropriate initial conditions such a pulse can form a black hole. Ours is the first study of the analogous process in Einstein-aether theory. In order to carry out the numerical simulations we developed the initial value formulation for this theory in spherical symmetry.

Here we have minimized the initial “distortion” of the aether field, by setting its divergence and acceleration to zero. (At the other extreme, one could study collapse of a pure spherical aether pulse, with no matter field at all.) These initial conditions are not precisely what would occur in an astrophysical setting, but should be indicative. We found that for the initial data studied, black holes with regular metric and spin-0 mode horizons form when the parameters in the Lagrangian are not too large. For larger parameters, a singularity occurs at finite area where the spin-0 horizon would have been. These results are consistent with findings from previous investigation of static solutions [29].

Since regular black holes have almost certainly been “observed” in nature, the black hole formation found here indicates that a strong-field test has been passed by ae-theory, at least for coupling parameters that are not so large that the spin-0 horizon is singular. Constraints from the absence of vacuum Čerenkov radiation require that the spin-0 mode travels at a speed greater than or equal to the “speed of light” as seen by matter fields [21], here the “metric” speed of light. Thus a the singular spin-0 horizon would necessarily be on or inside the matter horizon. Whether it could then have any observational consequences remains to be determined.

It would also be interesting and astrophysically important to examine the case of collapse with angular momentum, to a spinning black hole. The stationary spinning solutions have not yet been studied however,

and to follow the time-dependent collapse would require the general initial value formulation, without assuming hypersurface orthogonal aether nor spherical symmetry. In addition, axisymmetric codes are much more complicated.

Acknowledgments

This work was supported in part by the National Science Foundation under grants PHY-0601800 through the University of Maryland and PHY-0456655 through Oakland University.

APPENDIX: DERIVATION OF THE INITIAL VALUE FORMULATION FOR SPHERICALLY SYMMETRIC EINSTEIN-AETHER THEORY

In this section we derive the evolution equations for Einstein-aether theory in spherical symmetry. To begin with, we use only the hypersurface orthogonality of u^a and the Euler-Lagrange equations of motion (5-8).

Equation (6) (the equation of motion for the aether field) then becomes

$$c_{14} (\mathcal{L}_u a_a + 2K_{ab}a^b - Ka_a) + c_{13} D^b K_{ab} + c_2 D_a K = 0. \quad (\text{A.1})$$

Here \mathcal{L} denotes the Lie derivative and D_a is the spatial covariant derivative.

The usual initial value formulation for general relativity requires that we evolve h_{ab} and K_{ab} as well as the matter fields. From equation (20) we have

$$\mathcal{L}_u h_{ab} = -2K_{ab} \quad (\text{A.2})$$

which is used to evolve h_{ab} . The quantity K (the trace of K^a_b) satisfies the evolution equation

$$\mathcal{L}_u K = -D^a a_a - a^a a_a + K^{ab} K_{ab} + \frac{1}{2} T_{ab} (h^{ab} + u^a u^b). \quad (\text{A.3})$$

In addition, the quantity K_{ab} satisfies the constraint equation

$$D^b K_{ab} - D_a K = -h_a^b u^c T_{bc}. \quad (\text{A.4})$$

The extrinsic curvature K^a_b can be decomposed into a trace and a trace-free part. We will use equation (A.3) to evolve the trace K and will use equation (A.4) to find the trace-free part.

However, there is a subtlety associated with the Einstein-aether theory that makes the initial value problem somewhat complicated: the stress energy tensor contains terms that have second time derivatives of the aether field and second time derivatives of the metric. Thus after writing out the Einstein field equations one must solve them for these second time derivatives. In

particular, some straightforward but tedious algebra applied to equation (11) yields

$$T_{ab}(h^{ab} + u^a u^b) = -(c_{13} + 3c_2)\mathcal{L}_u K + c_{14}(D_a a^a + a_a a^a) + 2P^2 - 2c_{13}K_{ab}K^{ab} + c_{123}K^2 \quad (\text{A.5})$$

$$\begin{aligned} -h_a^b u^c T_{bc} &= -PD_a \psi \\ &- c_{14} (2K_{ab}a^b - Ka_a + \mathcal{L}_u a_a) \end{aligned} \quad (\text{A.6})$$

where $P = \mathcal{L}_u \psi$ and $c_{123} = c_1 + c_2 + c_3$. Using equation (A.5) in equation (A.3) and solving for $\mathcal{L}_u K$ yields

$$(2 + c_{13} + 3c_2) \mathcal{L}_u K = (c_{14} - 2)(D_a a^a + a_a a^a) + 2P^2 + 2(1 - c_{13})K_{ab}K^{ab} + c_{123}K^2. \quad (\text{A.7})$$

Similarly, equation (A.4), upon substituting the expression in equation (A.6), does not directly yield a constraint since the right hand side of equation (A.6) contains a term proportional to $\mathcal{L}_u a_a$. However, eliminating this term using equation (A.1) yields the following constraint

$$[1 - c_{13}]D^b K_{ab} = (1 + c_2)D_a K - PD_a \psi \quad (\text{A.8})$$

which can be used to rewrite the equation of motion for a_a as

$$\begin{aligned} \mathcal{L}_u a_a &= -2K_{ab}a^b + Ka_a + \frac{c_{13}}{c_{14}(1 - c_{13})} PD_a \psi \\ &- \frac{c_{123}}{c_{14}(1 - c_{13})} D_a K. \end{aligned} \quad (\text{A.9})$$

The usual Hamiltonian constraint of general relativity is

$${}^{(3)}R + K^2 - K^{ab}K_{ab} = 2T_{ab}u^a u^b \quad (\text{A.10})$$

where ${}^{(3)}R$ is the scalar curvature of the spatial metric. However, it follows from equation (11) that

$$\begin{aligned} 2T_{ab}u^a u^b &= 2c_{14}D_a a^a + P^2 + D_a \psi D^a \psi \\ &+ c_{14}a_a a^a - c_2 K^2 - c_{13}K_{ab}K^{ab}. \end{aligned} \quad (\text{A.11})$$

On substituting equation (A.11) into equation (A.10) one finds the constraint

$$\begin{aligned} {}^{(3)}R &= c_{14}(2D_a a^a + a_a a^a) + P^2 + D_a \psi D^a \psi \\ &+ (1 - c_{13})K_{ab}K^{ab} - (1 + c_2)K^2. \end{aligned} \quad (\text{A.12})$$

We now impose spherical symmetry. We use as a radial coordinate r the length in the radial direction (rather than an area coordinate). This makes the spatial metric

$$h_{ab} = \partial_a r \partial_b r + \Phi^2 \Sigma_{ab} \quad (\text{A.13})$$

where Σ_{ab} is the unit two-sphere metric. The time evolution vector field takes the form $t^a = \alpha u^a + \beta^a$. From the definition of P we find

$$\partial_t \psi = \alpha P + \beta^r \partial_r \psi \quad (\text{A.14})$$

while from the wave equation we obtain

$$\partial_t P = \beta^r \partial_r P + \alpha \left[PK + a^r \partial_r \psi + \partial_r \partial_r \psi + \frac{2\partial_r \Phi}{\Phi} \partial_r \psi \right]. \quad (\text{A.15})$$

It is helpful to define $Q \equiv K^r_r - (K/3)$ so that Q is the component of the trace-free part of K^a_b . From equation (A.2), we have the standard result

$$\mathcal{L}_t h_{ab} = -2\alpha K_{ab} + \mathcal{L}_\beta h_{ab}. \quad (\text{A.16})$$

The rr component of equation (A.16) yields

$$\partial_r \beta^r = \alpha(Q + K/3) \quad (\text{A.17})$$

while the $\theta\theta$ component yields

$$\partial_t \Phi = \beta^r \partial_r \Phi + \alpha \Phi (Q/2 - K/3). \quad (\text{A.18})$$

From the definition of α we have

$$\partial_r \ln \alpha = a_r. \quad (\text{A.19})$$

Equation (A.8) yields

$$\partial_r Q = -\frac{3Q}{\Phi} \partial_r \Phi + (1 - c_{13})^{-1} \left[\frac{1}{3}(2 + c_{13} + 3c_2) \partial_r K - P \partial_r \psi \right] \quad (\text{A.20})$$

while equations (A.9) and (A.7) yield respectively

$$\begin{aligned} \partial_t a_r &= \beta^r \partial_r a_r + \alpha \left[\left(\frac{2K}{3} - Q \right) a_r \right. \\ &\quad \left. + \frac{c_{13}}{c_{14}(1 - c_{13})} P \partial_r \psi - \frac{c_{123}}{c_{14}(1 - c_{13})} \partial_r K \right] \end{aligned} \quad (\text{A.21})$$

$$\begin{aligned} \partial_t K &= \beta^r \partial_r K + \frac{\alpha}{3} K^2 \\ &\quad + \frac{\alpha}{2 + c_{13} + 3c_2} \left[(c_{14} - 2)(\partial_r a_r + 2a_r \partial_r \Phi / \Phi + a_r a_r) \right. \\ &\quad \left. + 2P^2 + 3(1 - c_{13})Q^2 \right]. \end{aligned} \quad (\text{A.22})$$

The Hamiltonian constraint (equation (A.12)) becomes the vanishing of the quantity \mathcal{C} where

$$\begin{aligned} \mathcal{C} &= \partial_r \partial_r \Phi + \frac{(\partial_r \Phi)^2 - 1}{2\Phi} + c_{14} a_r \partial_r \Phi \\ &\quad + \frac{\Phi}{4} \left[c_{14}(2\partial_r a_r + a_r a_r) + P^2 + (\partial_r \psi)^2 \right. \\ &\quad \left. + \frac{3}{2}(1 - c_{13})Q^2 - \frac{1}{3}(2 + c_{13} + 3c_2)K^2 \right]. \end{aligned} \quad (\text{A.23})$$

-
- [1] D. Mattingly, “Modern tests of Lorentz invariance,” *Living Rev. Rel.* **8**, 5 (2005) [arXiv:gr-qc/0502097].
- [2] C.M. Will and K. Nordtvedt, Jr., “Conservation Laws and Preferred Frames in Relativistic Gravity. I. Preferred-Frame Theories and an Extended PPN Formalism,” *Astrophys. J.* **177**, 757 (1972); K. Nordtvedt, Jr. and C.M. Will, “Conservation Laws and Preferred Frames in Relativistic Gravity. II. Experimental Evidence to Rule Out Preferred-Frame Theories of Gravity,” *Astrophys. J.* **177**, 775 (1972); R.W. Hellings and K. Nordtvedt, Jr., “Vector-metric theory of gravity,” *Phys. Rev. D* **7**, 3593 (1973).
- [3] M. Gasperini, “Classical Repulsive Gravity and Broken Lorentz Symmetry,” *Phys. Rev. D* **34**, 2260 (1986).
- [4] V. A. Kostelecky and S. Samuel, “Gravitational phenomenology in higher dimensional theories and strings,” *Phys. Rev. D* **40**, 1886 (1989).
- [5] M. A. Clayton and J. W. Moffat, “Scalar-Tensor Gravity Theory For Dynamical Light Velocity,” *Phys. Lett. B* **477**, 269 (2000) [arXiv:gr-qc/9910112].
- [6] T. Jacobson and D. Mattingly, “Gravity with a dynamical preferred frame,” *Phys. Rev. D* **64**, 024028 (2001) [arXiv:gr-qc/0007031].
- [7] N. Arkani-Hamed, H. C. Cheng, M. A. Luty and S. Mukohyama, “Ghost condensation and a consistent infrared modification of gravity,” *JHEP* **0405**, 074 (2004) [arXiv:hep-th/0312099].
- [8] J. D. Bekenstein, “Relativistic gravitation theory for the MOND paradigm,” *Phys. Rev. D* **70**, 083509 (2004) [Erratum-ibid. *D* **71**, 069901 (2005)] [arXiv:astro-ph/0403694].
- [9] B. M. Griopoulos, “Modified gravity via spontaneous symmetry breaking,” *JHEP* **0410**, 069 (2004) [arXiv:hep-th/0408127].
- [10] R. Bluhm and V. A. Kostelecky, “Spontaneous Lorentz violation, Nambu-Goldstone modes, and gravity,” *Phys. Rev. D* **71**, 065008 (2005) [arXiv:hep-th/0412320].
- [11] C. Heinicke, P. Baekler and F. W. Hehl, “Einstein-aether theory, violation of Lorentz invariance, and metric-affine gravity,” *Phys. Rev. D* **72**, 025012 (2005) [arXiv:gr-qc/0504005].
- [12] V. A. Rubakov, “Phantom without UV pathology,” arXiv:hep-th/0604153.
- [13] H. C. Cheng, M. A. Luty, S. Mukohyama and J. Thaler, “Spontaneous Lorentz breaking at high energies,” *JHEP* **0605**, 076 (2006) [arXiv:hep-th/0603010].
- [14] T. G. Zlosnik, P. G. Ferreira and G. D. Starkman, “Modifying gravity with the aether: An alternative to dark matter,” arXiv:astro-ph/0607411.
- [15] C. Eling, T. Jacobson and D. Mattingly, “Einstein-aether theory,” in *Deserfest*, eds. J. Liu, M. J. Duff, K. Stelle, and R. P. Woodard (World Scientific, 2006) arXiv:gr-qc/0410001.
- [16] C. Eling and T. Jacobson, “Static post-Newtonian equivalence of GR and gravity with a dynamical preferred frame,” *Phys. Rev. D* **69**, 064005 (2004) [arXiv:gr-qc/0310044].
- [17] M. L. Graesser, A. Jenkins and M. B. Wise, “Spontaneous Lorentz violation and the long-range gravitational preferred-frame effect,” *Phys. Lett. B* **613**, 5 (2005) [arXiv:hep-th/0501223].
- [18] B. Z. Foster and T. Jacobson, “Post-Newtonian param-

- eters and constraints on Einstein-aether theory,” *Phys. Rev. D* **73**, 064015 (2006) [arXiv:gr-qc/0509083].
- [19] T. Jacobson and D. Mattingly, “Einstein–Aether waves,” *Phys. Rev. D* **70**, 024003 (2004) [arXiv:gr-qc/0402005].
- [20] E. A. Lim, “Can We See Lorentz-Violating Vector Fields in the CMB?,” *Phys. Rev. D* **71**, 063504 (2005) [arXiv:astro-ph/0407437].
- [21] J. W. Elliott, G. D. Moore and H. Stoica, “Constraining the new aether: Gravitational Cherenkov radiation,” *JHEP* **0508**, 066 (2005) [arXiv:hep-ph/0505211].
- [22] C. Eling, “Energy in the Einstein-aether theory,” *Phys. Rev. D* **73**, 084026 (2006) [arXiv:gr-qc/0507059].
- [23] S. M. Carroll and E. A. Lim, “Lorentz-violating vector fields slow the universe down,” *Phys. Rev. D* **70**, 123525 (2004) [arXiv:hep-th/0407149].
- [24] B. Z. Foster, “Radiation damping in Einstein-aether theory,” *Phys. Rev. D* **73**, 104012 (2006) [arXiv:gr-qc/0602004].
- [25] B. Z. Foster, in preparation.
- [26] S. Mukohyama, “Black holes in the ghost condensate,” *Phys. Rev. D* **71**, 104019 (2005) [arXiv:hep-th/0502189].
- [27] D. Giannios, “Spherically symmetric, static spacetimes in TeVeS,” *Phys. Rev. D* **71**, 103511 (2005) [arXiv:gr-qc/0502122].
- [28] C. Eling and T. Jacobson, “Spherical Solutions in Einstein-aether Theory: Static Aether and Stars,” *Class. Quant. Grav.* **23**, 5625 (2006) [arXiv:gr-qc/0603058].
- [29] C. Eling and T. Jacobson, “Black holes in Einstein-Aether theory,” *Class. Quant. Grav.* **23**, 5643 (2006) [arXiv:gr-qc/0604088].
- [30] B. Z. Foster, “Metric redefinitions in Einstein-aether theory,” *Phys. Rev. D* **72**, 044017 (2005) [arXiv:gr-qc/0502066].